Cell Type and Culture Condition–Dependent Alternative Splicing in Human Breast Cancer Cells Revealed by Splicing-Sensitive Microarrays

Chunxia Li,[1,2] Mitsuo Kato,[2] Lily Shiue,[4] John E. Shively,[1,3] Manuel Ares, Jr.,[4] and Ren-Jang Lin[1,2]

[1]City of Hope Graduate School of Biological Sciences; Divisions of [2]Molecular Biology and [3]Immunology, Beckman Research Institute of City of Hope, Duarte, California; and [4]Department of Molecular, Cell and Developmental Biology, University of California, Santa Cruz, California

Abstract

Growing evidence indicates that alternative or aberrant pre-mRNA splicing takes place during the development, progression, and metastasis of breast cancer. However, which splicing changes that might contribute directly to tumorigenesis or cancer progression remain to be elucidated. We used splicing-sensitive microarrays to detect differences in alternative splicing between two breast cancer cell lines, MCF7 (estrogen receptor positive) and MDA-MB-231 (estrogen receptor negative), as well as cultured human mammary epithelial cells. Several splicing alterations in genes, including *CD44, FAS, RBM9, hnRNPA/B, APLP2*, and *MYL6*, were detected by the microarray and verified by reverse transcription-PCR. We also compared splicing in these breast cancer cells cultured in either two-dimensional flat dishes or in three-dimensional Matrigel conditions. Only a subset of the splicing differences that distinguish MCF7 cells from MDA-MB-231 cells under two-dimensional culture condition is retained under three-dimensional conditions, suggesting that alternative splicing events are influenced by the geometry of the culture conditions of these cells. Further characterization of splicing patterns of several genes in MCF7 cells grown in Matrigel and in xenograft in nude mice shows that splicing is similar under both conditions. Thus, our oligonucleotide microarray can effectively detect changes in alternative splicing in different cells or in the same cells grown in different environments. Our findings also illustrate the potential for understanding gene expression with resolution of alternative splicing in the study of breast cancer. (Cancer Res 2006; 66(4): 1990-9)

Introduction

Alternative splicing is a key posttranscriptional mechanism by which the expression of multiple protein products from a single gene can be controlled. Accumulating lines of evidence indicate that alternative splicing is changed or becomes aberrant during the development, progression, and metastasis of breast cancer. For example, unusual splice variants of several genes, including estrogen receptors (*ER*), prolactin receptors, *BRCA1, CD44, Her2/neu, AIB-1,* and growth factor receptors, have been detected in breast cancer cell lines or tumor tissues (1). Little is known about the relationship between changes in splicing and other events during the progression of breast cancer.

Mutations in *cis*-acting splicing elements could cause changes in constitutive or alternative splicing in specific key genes during development of breast cancer. For example, germ line mutations in the breast cancer susceptibility gene *BRCA1* lead to predisposition to breast cancer and ovarian cancer (2, 3). A G-to-T transversion mutation at nucleotide 5,199 in exon 18 of the *BRCA1* gene was found in a number of patients, including eight cases of breast and ovarian cancer within a family (4). This mutation leads to the skipping of exon 18 in the *BRCA1* gene, probably by altering an exonic splicing enhancer (5). Skipping exon 18 results in the removal of 26 amino acids in a region essential for the DNA repair, transcriptional regulation, and tumor suppressor functions of BRCA1 (4). Thus, mutations that occurred in *cis*-acting splicing elements could alter the splicing of genes that are important for control of cell growth.

Changes in alternative splicing during breast cancer could also be mediated through changes in *trans*-acting splicing factors, such as the serine-arginine–rich (SR) proteins (6, 7). SR proteins contain RS repeats and RNA recognition motifs and play important roles in both constitutive splicing and regulated alternative splicing. Stepwise increases in expression of several SR proteins have been shown to occur during mammary gland development and tumorigenesis in a mouse model (8). The study showed that the amount of these SR proteins started to increase during early preneoplasia and the increase became more pronounced during tumor formation (8). Thus, the changes of SR protein expression could lead to changes of alternative splicing in breast cancer.

To begin to understand the role of alternative splicing in breast cancer progression, we sought a broad systematic approach to simultaneously detect splicing alterations in many genes. Microarray-based techniques to detect a large number of splicing events in yeast, *Drosophila*, and vertebrate systems have been reported (9–17). We developed and tested a splicing-sensitive microarray with exon and splice junction oligonucleotides to assay splicing of a number of human genes implicated in cancer progression and apoptosis. As a first step, we compared the MCF7 and the MDA-MB-231 breast cancer cell lines with cultured human mammary epithelial cells (HMEC). MCF7 cells, established from a pleural effusion, express ER and are estrogen-responsive breast cancer cells. MCF7 cells do not form metastases in nude mice unless estrogen supplementation is provided (18, 19). MDA-MB-231 cells were also established from a pleural effusion; however, these cells are ER-negative and highly invasive. I.v. injection of MDA-MB-231 cells into the tail vein of nude mice produces tumors (18). Here, we report changes in alternative splicing in MCF7 and MDA-MB-231 cells compared with HMEC and with each other. In addition, we found differences within cell types when grown in different

Note: Supplementary data for this article are available at Cancer Research Online (http://cancerres.aacrjournals.org/).

Requests for reprints: Ren-Jang Lin, Division of Molecular Biology, Beckman Research Institute of City of Hope, 1450 East Duarte Road, Duarte, CA 91010. Phone: 626-301-8286; Fax: 626-301-8280; E-mail: rlin@coh.org.

doi:10.1158/0008-5472.CAN-05-2593

conditions such as flat dishes (two dimensional), Matrigel (three dimensional), and in nude mice as xenografts. The results illustrate the potential of using oligonucleotide microarrays for measuring gene expression with resolution of alternative splicing in the study of breast cancer progression.

Materials and Methods

Cell culture. Cells (two-dimensional cultures) were grown in flat dishes as follows: HMEC cells (Clonetics, San Diego, CA) were cultured in mammary epithelial cell growth medium (MEGM; Clonetics) supplemented with 10% fetal bovine serum (FBS; HyClone, Logan, UT) and MEGM bullet kit (Clonetics), which contains 10 ng/mL hEGF, 5 μg/mL insulin, 0.5 μg/mL hydrocortisone, 50 μg/mL gentamicine, 50 ng/mL amphotericin-B, and 52 μg/mL bovine pituitary extract. MCF7 cells [American Type Culture Collection (ATCC), Manassas, VA] were cultured in DMEM (Mediatech, Herndon, VA) supplemented with 10% FBS, 1% nonessential amino acids (Irvine Scientific, Santa Ana, CA), and 1% penicillin/streptomycin (Irvine Scientific). MDA-MB-231 cells (ATCC) were cultured in RPMI 1640 with L-glutamine (Irvine Scientific) supplemented with 10% FBS and 1% penicillin/streptomycin. To grow cells in Matrigel, cells were first grown in dishes, harvested, resuspended, and 6.0×10^5 cells were embedded in a 1-mm-thick layer of Matrigel basement membrane matrix (BD Clontech, Mountain View, CA) in six-well plates. Solidified Matrigel at 37°C was overlaid with MEGM growth medium. To harvest cells, gels were incubated in 2 mL cell recovery solution (BD Clontech) for 1 hour at 4°C and centrifuged at $200 \times g$ to $300 \times g$ for 5 minutes at 4°C.

MCF7 xenografts. Female, athymic *nu/nu* mice (Charles River, Wilmington, MA), 10 to 12 weeks old, were exposed to 200 rad external beam Co-60 irradiation 3 days before MCF7 implantation and were given Sulfatrim antibiotic water for 2 weeks. Two days before MCF7 implantation, 0.8 mg Delestrogen was administered to mice via i.m. injection into the thigh. MCF7 cells cultured in DMEM in dishes were harvested and implanted s.c. in the flank of each mouse. Tumors developed within 10 to 14 days postinjection.

RNA extraction. Total RNA was extracted from cells or homogenized xenograft using TRIzol reagent (Invitrogen, Carlsbad, CA) according to the protocol of the manufacturer. For xenograft, 0.2 g sample was homogenized in 3 mL TRIzol in a 7 mL glass homogenizer (Wheaton, Millville, NJ) for 10 minutes. The homogenized sample was centrifuged and RNA was extracted from the supernatant. The quality of RNA was checked by running 2 μg on a 1% denaturing agarose gel; the intensity of the 28S rRNA and 18S rRNA bands were measured and the ratio between them was between 1.60 and 1.82. The RNA sample was treated with DNase I, followed by phenol/chloroform extraction, before being used in reverse transcription reaction.

Microarray design and production. The principle of oligonucleotide selection and the design of microarray have been described previously (9). Briefly, 5′ amino-linker containing oligonucleotides were printed and covalently attached through the 5′ amino group onto Codelink slides (Amersham, Piscataway, NJ). Printing was done by a robotic contact pin printer essentially as described by the Brown lab at Stanford University.[5]

Fluorescent labeling and hybridization in microarray. Synthesis of fluorescently labeled cDNA was carried out at 42°C for 2 hours in a 30 μL reaction containing 20 μg total RNA, 5 μg oligo(dT) (Invitrogen), 1 μg random hexamers (Ambion, Austin, TX), 3 μL of 10× deoxynucleotide triphosphate (dNTP) mix (25 mmol/L dGTP, 25 mmol/L dATP, 25 mmol/L dCTP, 15 mmol/L dTTP, and 10 mmol/L aminoallyl-dUTP), and 2 μL of 200 units/μL SuperScript Reverse Transcriptase (Invitrogen). The cDNA synthesized was subsequently chemically coupled to either Cy3 or Cy5 fluorescent dyes (Amersham Pharmacia, Piscataway, NJ) through incubation with 2 μL dye in the dark room at room temperature for 1 hour. After purification using QIAquick PCR purification kit (Qiagen, Valencia, CA), the Cy3- and Cy5-labeled cDNA probes were combined and concentrated in SpeedVac (Savant, Holbrook, NY); 10 μL was then mixed with 10 μL of 2× hybridization buffer (8× SSC, 0.2% SDS, and 0.2 μg/μL polyadenylic acid; Sigma, St. Louis, MO) and applied to the oligospotted area on the slide that was covered by a LifterSlip (Erie Scientific, Portsmouth, NH). Hybridization was carried out in a 62°C water bath overnight in a hybridization chamber (TeleChem International, Sunnyvale, CA). The slide was washed at room temperature twice with 2× SC, 0.1% SDS for 5 minutes, once with 0.2× SSC for 1 minute, and once with 0.05× SSC for 1 minute. Hybridization signals were determined by scanning the slide using a scanning laser microscope Axon 4000 B at 635 nm (for Cy5 red dye) and 532 nm (for Cy3 green dye) and GenePix Pro 4.1 software (Axon Instruments, Union City, CA).

Microarray data analysis. Oligonucleotide spots with both F635 and F532 readings below average plus two SD values of all "untargeted" spots were removed from the raw data. "Untargeted" spots were oligonucleotides with sequences not found in the human genome or containing only printing buffer. The F635/F532 ratio was then calculated for each spot and the mean of all spots with the same sequence (typically a total of eight measurements) was calculated. The value was adjusted by using 40th percentile whole-chip normalization. Data were analyzed with GeneSpring software version 6.1 (Silicon Genetics, Redwood City, CA). The data set was exported to Microsoft Excel for further analysis. The skipping index was calculated by taking $\log_2$ of the ratio between exon-skipping junction (e.g., e1-e2 in Fig. 1*A*) and constitutive exon, whereas the inclusion index was calculated using exon-inclusion junction (e.g., e1-a1 in Fig. 1*A*) and constitutive exon. One and a half–fold changes in either direction (>0.58 or less than −0.58 of the index) were arbitrarily chosen as cutoff.

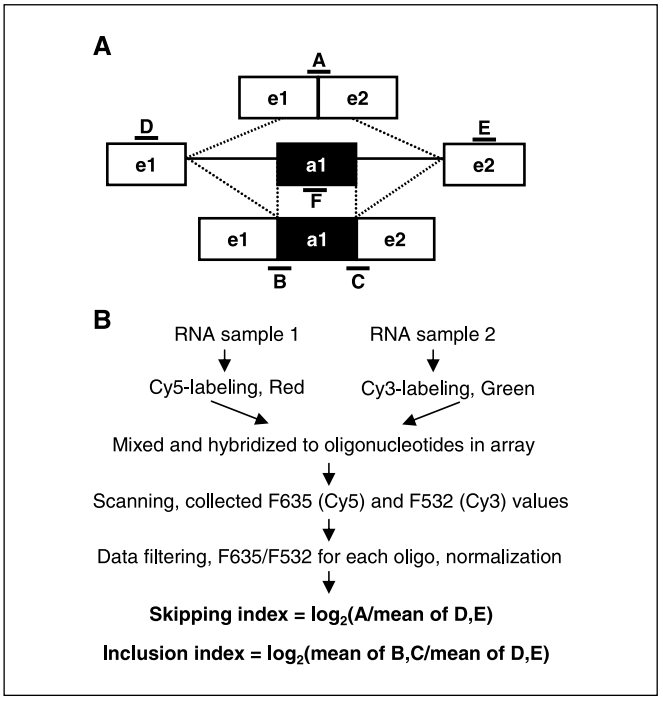

Figure 1. Detection of alternative splicing by splicing-sensitive microarray. *A*, design of oligo probes. The microarray probes contain 40-mer oligonucleotides that target exon-exon junction sequences because different alternative splice forms have distinct exon-exon junctions. Probes A, B, and C span distinct exon-exon junctions; probes D and E are complementary to flanking constitutive exons (e1 and e2); probe F is complementary to alternative exon a1. *B*, data collection and analysis. RNA samples 1 and 2 were isolated and labeled separately with Cy5 or Cy3 fluorescent dye, mixed, and hybridized to oligonucleotides in microarray on a slide. Red (F635) and green (F532) fluorescence were measured and the ratio of the two values was calculated for each oligonucleotide. To access differences in splicing pattern between the two samples, skipping indexes and inclusion indexes were calculated. The skipping index of alternative exon a1 is $\log_2$ of F635/F532 from the e1-e2 junction oligonucleotide (probe A in *A*) divided by the mean of F635/F532 from the constitutive exons e1 and e2 (probes D and E in *A*). The inclusion index of a1 is $\log_2$ of the mean of F635/F532 from e1-a1 and a1-e2 (probes B and C in *A*) divided by the mean of F635/F532 from e1 and e2 (probes D and E in *A*).

[5] http://cmgm.stanford.edu/pbrown/mguide/index.html.

Reverse transcription-PCR. cDNA was synthesized in 20 μL reaction containing 5 μg total RNA, 1 μg oligo(dT), 0.2 μg random hexamers, 2 μL of 10× dNTP mix (25 mmol/L each of dGTP, dATP, dCTP, and dTTP), and 1 μL of 200 units/μL SuperScript Reverse Transcriptase. PCR was carried out in 50 μL reaction containing 1 μL of the synthesized cDNA in 30 cycles of 30 seconds at 94°C, 30 seconds at the melting temperature (T_m) of the primers, and 30 to 60 seconds depending on the product size (60 seconds for 1 kb) at 72°C. Products were resolved on a 2% agarose gel in Tris-borate EDTA buffer. Primers and their T_m are listed in Supplementary Table S2. Band intensity was quantitated using Bio-Rad Gel Doc 2000 (Bio-Rad, Hercules, CA).

Results

Splicing-sensitive microarrays. To investigate differences in alternative splicing, we used a customized oligonucleotide splicing-sensitive microarray (20). Figure 1*A* illustrates the design of oligonucleotides for the detection of splicing variants from a given gene. For example, oligonucleotide A, B, or C consists of exon-exon junction sequence and different splice variants will have different exon-exon junctions. The microarray also contains oligonucleotides D, E, and F, which are complementary to flanking constitutive exons e1 and e2, and the alternative exon a1. This splicing-sensitive microarray was used because a signal derived from the hybridization to the constitutive exon oligonucleotides (e1 or e2) would, in theory, reflect the total amount of RNA from the particular gene, whereas hybridization signals from an exon-exon junction oligonucleotide would reflect the amount of RNA containing that particular junction. The ratio of hybridization intensity from an oligonucleotide spanning a specific exon-exon junction to that from a constitutive exon oligonucleotide would provide information about the level of that alternatively spliced RNA in the two comparison samples (9). Using this type of splicing-sensitive array, one can acquire two sets of information from one array: expression level changes for the gene and changes in the distribution of the splice variants.

The array used in this study contained 64 genes (Supplementary Data) that underwent alternative splicing, including *ERα* and *ERβ*, *CD44* (cell adhesion molecule), *ITGA6* (integrin α6 precursor), *FAS*, *LARD*, *WT1* (Wilms' tumor protein 1), and *TP73* (tumor suppressor p73). Each gene could contain one or more simple alternative exons or more complex arrangements of multiple alternative exons. We chose these 64 genes by two methods (20). The first method was that they were reported to change in their alternative splicing during cancer or were genes with alternative splicing that play a role in cancer. The second group was chosen to be well expressed in four human cell lines on an Affymetrix expression array and for which good evidence of alternative splicing existed in the University of California Santa Cruz genome browser. The splicing changes we examined in the 64 genes included simple exon inclusion or skipping and complex multiple alternative exons (20). In all cases, the splice variants have been described in expressed sequence tag databases or in publications because they have to be known to be designed on the array. Many splice variants are in frame but some are out of frame; these are possible in part because they are observed in cancer cell lines, which could be altered in nonsense-mediated decay or otherwise deregulated.

Figure 1*B* briefly describes the procedure in splicing microarray analysis. RNA samples were isolated and labeled separately with Cy5 or Cy3 fluorescent dye, mixed, and hybridized to oligonucleotides in microarray on a slide. Red (F635) and green (F532) fluorescence were measured and the ratio of the two values was calculated for each oligonucleotide. To access differences in splicing pattern between the two samples, skipping indexes and inclusion indexes were calculated (Fig. 1*B*). The skipping index of alternative exon a1 is $\log_2$ of F635/F532 from the e1 to e2 junction oligonucleotide divided by the mean of F635/F532 from the constitutive exons e1 and e2.

$$\text{Skipping index} = \log_2[A_{\text{sample 1}}/A_{\text{sample 2}}] - \log_2[\text{mean of } (D_{\text{sample 1}}/D_{\text{sample 2}} \text{ and } E_{\text{sample 1}}/E_{\text{sample 2}})]$$

The inclusion index of a1 is $\log_2$ of the mean of F635/F532 from e1 to a1 and a1 to e2 divided by the mean of F635/F532 from e1 and e2.

$$\text{Inclusion index} = \log_2[\text{mean of } (B_{\text{sample 1}}/B_{\text{sample 2}} \text{ and } C_{\text{sample 1}}/C_{\text{sample 2}})] - \log_2[\text{mean of } (D_{\text{sample 1}}/D_{\text{sample 2}} \text{ and } E_{\text{sample 1}}/E_{\text{sample 2}})]$$

Genes with a skipping or inclusion index larger than 0.58 (1.5-fold higher) or smaller than −0.58 (1.5-fold lower) were arbitrarily chosen for further analysis by reverse transcription-PCR (RT-PCR) to examine their splice variants. Results from both assays were compared where possible.

Splicing differences between breast cancer cells and mammary epithelial cells. To begin examining changes of alternative splicing in breast cancer, we compared the alternative splicing in MCF7 and MDA-MB-231 breast cancer cells with the alternative splicing in cultured HMECs. Total RNA was extracted from cells cultured in flat dishes, converted to cDNA, and labeled with Cy3 (green) or Cy5 (red) fluorescent dye. A Cy3-labeled MCF7 sample was combined with an equal amount of a Cy5-labeled HMEC sample and hybridized to oligonucleotides on a microarray slide. A reciprocal experiment using Cy5-MCF7 and Cy3-HMEC was also carried out. After scanning slides, data were filtered, normalized, and combined to obtain the inclusion index and the skipping index for the alternative splicing events. We found 15 alternative splicing events that vary >1.5-fold between the two samples (i.e., at least one of the two splicing indexes was >0.58 or less than −0.58; Table 1). We also carried out a similar microarray analysis to compare the RNA samples from MDA-MB-231 and HMEC cells and we found 17 alternative splicing events that had at least one splicing index changed by 0.58 (Table 2).

In Table 1, a positive inclusion index (e.g., MAP4K4) indicated that the mRNA containing the alternative exon was present at a relatively higher level in MCF7 than in HMEC; a positive skipping index (e.g., MYL6) indicated that the mRNA lacking the alternative exon was present at a relatively higher level in MCF7 than in HMEC. Likewise, a negative inclusion index indicated relatively less inclusion and a negative skipping index indicated relatively less exclusion in MCF7. In a number of cases, a positive inclusion index of an alternative exon was not accompanied by a significant negative skipping index of the same exon (Tables 1 and 2), suggesting that either the two splice forms were quite different in quantity or other processes like RNA stability were involved. There were three cases where a change of one index was concomitant with a change of the other index in the opposite direction (MYL6 and DDR1 in Table 1; CD44 exon v8 in Table 2). Paradoxically, there were four cases where both indexes changed in the same direction (CD44 exon v10 in Tables 1 and 2; CD44 exon v8 in Table 1; and TPD52L1 in Table 2). These four cases most likely resulted from the

Table 1. Splicing indexes of MCF7/HMEC

Gene	Alternative exon		Splicing index		RT-PCR confirmation
	Name	Length (nt)	Inclusion	Skipping	
MAP4K4	Exon 17	231	1.29	0.27	Yes
VEGF	Exon 6	72	0.94	0.20	Yes
MYL6	Exon 6	45	−0.96	0.92	Yes
DDR1	Exon 8	168	−0.64	0.86	Yes
FAS	Exons 3, 4	109, 109	0.07	2.25	Yes
ZNF207	Exon 9	93	0.01	0.89	Yes
hnRNPA/B	Exon 7	141	−0.28	−0.99	Yes
APLP2	Exon 7	168	−0.06	−0.65	Yes
RBM9	Exon 9	145	−0.01	−0.59	Yes
CD44	Exon 14 or v10	204	0.89*	1.06†	Yes
CD44	Exon 12 or v8	102	1.27‡	1.06†	Yes
CASP3	Exon 6	121	0.56	1.06	No
CKLF1	Exons 2, 3	159, 96	0.30	0.71	No
KARS	Exon 2	180	0.23	−0.61	No
MYLK	Exon 10	204	−0.36	1.18	No

Abbreviation: nt, nucleotide.
*Oligo probe e5-v10 (see Fig. 5).
†Oligo probe e5-e15 (see Fig. 5).
‡Oligo probe e5-v8 (see Fig. 5).

fact that both genes have multiple alternative exons that can be spliced in a complex manner (21, 22). For example, human CD44 has nine variable exons that could be included or excluded in various combinations. Thus, the sum of all splice variants of CD44 that include a specific variable exon and the sum of all splice variants that exclude that specific variable exon could simultaneously increase with a decrease of other splice variants (see below).

To evaluate the accuracy of the microarray and to analyze complex splicing variants (as in the case of CD44), we carried out RT-PCR using flanking primers to examine those RNA samples (examples are shown below). Among the 15 splicing differences between MCF7 and HMEC, 11 were revealed by RT-PCR (Table 1); among the 14 splicing differences between MDA-MB-231 and HMEC that were analyzed by RT-PCR, 11 were detected by the assay (Table 2). Thus, 75% (22 of 29) of the splicing changes revealed by the microarray, using the 1.5-fold cutoff, were confirmed by RT-PCR. Therefore, our oligonucleotide microarray was effective in measuring changes in alternative splicing in breast cancer cell lines.

Splicing patterns of MCF7 and MDA-MB-231 cells grown in dishes or in Matrigel. We further analyzed the differences in alternative splicing in the two breast cancer cell lines by comparing them directly with each other using microarrays. We particularly wanted to investigate how culture conditions affect splicing patterns. We compared splicing differences in MCF7 and MDA-MB-231 cells cultured in two-dimension (flat dishes) and in three-dimension (Matrigel). Matrigel is a solubilized basement membrane matrix extracted from the Engelbreth-Holm-Swarm mouse sarcoma, which contains extracellular matrix proteins, such as laminin and collagen IV, and mimics the extracellular matrix (23). Patterns of gene expression and other biological activities in cells grown in three-dimensional culture conditions more closely mirror those found in living organisms (24–26); thus, we were interested in comparing splicing.

The MDA-MB-231 cells seemed to have a spindle shape with epithelial-like morphology when grown on flat dish (the two-dimensional condition; Fig. 2*A*), whereas in Matrigel (the three-dimensional condition) they formed large colonies with cells connected in a network (Fig. 2*B*). The observation was similar to what has been reported previously (27). The MCF7 cells showed typical round spindle-shaped epithelial cell morphology when cultured in flat dish (Fig. 2*C*), and in Matrigel they developed into solid spheres (Fig. 2*D*) as what we have previously described (28).

In pilot studies, we found, by RT-PCR, no splicing differences in CD44, FAS, or DNMT3B among cells of the same cell line cultured in Matrigel for 5, 7, 9, or 12 days (data not shown). Therefore, we chose day 7 to extract RNA from MCF7 and MDA-MB-231 cells cultured in Matrigel and did the splicing-sensitive microarray analysis. For flat dish–grown cells, RNA was extracted after 3 days of culturing. Fifteen splicing changes with at least one splicing index >0.58 or smaller than −0.58 were found when comparing two-dimensional grown cells (Table 3). Seven differences were retained in cells grown three-dimensionally, whereas eight differences became insignificant (Table 3). We also carried out RT-PCR to look at splice variants from 12 of the 15 genes in those two sets of RNA samples (data not shown; see Figs. 3-6 for examples). The results from the RT-PCR assay agreed with the microarray results in 19 of 24 cases (Table 3). In the case of vascular endothelial growth factor (VEGF), both assays indicated that the alternative exon (exon 6) was included less frequently in MDA-MB-231 cells in two-dimensional comparison. In the three-dimensional comparison, the microarray showed VEGF having an inclusion index of −0.54, which was slightly below the cutoff, whereas RT-PCR detected significant decrease in exon 6 inclusion in MDA-MB-231 cells. In the cases of BCL2L1 and MYLK, the microarray results were not confirmed by RT-PCR. Nevertheless, the agreements between the two assays were nearly 80% (19 of 24).

The results shown in Table 3 indicated that alternative splicing differed in 10 genes between these two breast cancer cell lines when cultured in flat dishes. However, four of these splicing events were no longer significantly different and only six splicing differences (including VEGF) were found when the cell lines were cultured in Matrigel. Thus, alternative splicing is likely influenced by the culture conditions and different cell lines could respond in different ways with respect to splicing regulation.

The two-dimensional and three-dimensional cultures differed not only in geometry but also in the growth medium used. To investigate how much the growth medium contributed to the change of splicing, we first cultured the MCF7 and MDA-MB-231 cells in flat dish with their own medium, and upon dilution plated them either in the original medium or in the MEGM medium that were used in Matrigel culture. After the cells reached 75% confluence, RNA was extracted from the cells and splicing of several RNAs was assayed by RT-PCR (Supplementary Data). In both cases, RT-PCR did not detect significant splicing changes in the same cell line grown in two different media, suggesting that medium ingredients, such as growth factors used in Matrigel culturing, contributed little to the observed splicing differences. Thus, the cell-to-matrix or cell-to-cell contact is more likely to cause the splicing differences between cells cultured two-dimensionally or three-dimensionally. Because HMEC cells were always cultured in MEGM medium, this result also suggested that the splicing differences we detected between HMEC cells and the two cancer cell lines (Tables 1 and 2) was not caused mainly by the difference in culture medium.

Further characterization of alternatively spliced RNAs from three genes. APLP2, known as amyloid β (A4) precursor-like protein 2, is a transmembrane glycoprotein associated with Alzheimer's disease (29) and is recently shown to be involved in neuroblastoma (30). APLP2 has an alternative exon 7 of 168 nucleotides encoding the Kunitz protease inhibitor domain (31), and alternative splicing would result in two different proteins, either lacking or containing the entire Kunitz protease inhibitor domain. Microarray results indicated that, when comparing to HMEC cells, MCF7 cells had less skipped form of APLP2 (Table 1) whereas MDA-MB-231 cells had less inclusion form (Table 2).

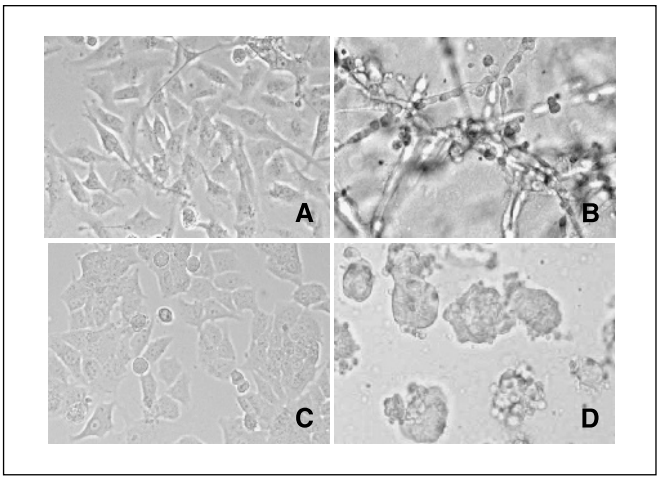

Figure 2. Morphologic differences of two-dimensional and three-dimensional cell cultures. MDA-MB-231 cells cultured in two-dimensional flat dishes for 3 days (*A*) or cultured in Matrigel for 7 days (*B*). MCF7 cells cultured in two-dimensional flat dish for 3 days (*C*) or cultured in Matrigel for 7 days (*D*). Magnification, ×10.

Table 2. Splicing indexes of MDA-MB-231/HMEC

Gene	Alternative exon		Splicing index		RT-PCR confirmation
	Name	Length (nt)	Inclusion	Skipping	
HRMT1L1	Exon 2	109	0.76	−0.07	Yes
MYL6	Exon 6	45	−1.21	0.22	Yes
SCML1	Exons 3, 4	149, 84	−0.69	0.04	Yes
APLP2	Exon 7	168	−0.59	0.32	Yes
FAS	Exons 3, 4	109, 109	0.17	1.22	Yes
ESR1	Exon 4	139	0.09	0.76	Yes
hnRNPA/B	Exon 7	141	−0.14	−2.17	Yes
RBM9	Exon 9	145	0.20	−0.58	Yes
CD44	Exon 14 or v10	204	0.74*	1.86 †	Yes
CD44	Exon 12 or v8	102	−0.64 ‡	1.86 †	Yes
TPD52L1	Exons 5, 6	39, 61	−1.29	−1.16	Yes
STK6	Exon 2	98	−0.65	−0.01	NA§
HTATIP	Exon 5	156	0.23	0.62	No
ESR2	Exon 11	139	0.18	0.84	No
TPM2	Exon 6	76	0.79	0.23	ND
TP73	Exon 13	94	0.04	1.00	ND
ITGA6	Exon 25	130	−0.32	1.00	ND

Abbreviations: N/A, not applicable; ND, not done.
*Oligo probe e5-v10 (see Fig. 5).
†Oligo probe e5-E15 (see Fig. 5).
‡Oligo probe e5-v8 (see Fig. 5).
§Alu repeat sequences.

Table 3. Splicing changes for MDA-MB-231 versus MCF7 cells cultured in two-dimensional and three-dimensional conditions

Gene	Alternative exon		Splicing index (two-dimensional)		RT-PCR confirmation	Splicing index (three-dimensional)		RT-PCR confirmation
	Name	Length (nt)	Inclusion	Skipping		Inclusion	Skipping	
HRMT1L1	Exon 2	109	0.86	−0.32	Yes	0.80	−0.03	Yes
APLP2	Exon 7	168	−1.15	0.65	Yes	−1.00	1.01	Yes
CD44	Exon 12 or v8	102	−1.84*	0.14 †	Yes	−1.00*	0.33 †	Yes
VEGF	Exon 6	72	−0.69	−0.18	Yes	−0.54	−0.06	No
ESR1	Exon 4	139	0.15	2.98	Yes	0.48	1.84	Yes
EEF1D	Exon 3	72	−0.18	0.83	Yes	−0.25	0.96	Yes
TPD52L1	Exons 5, 6	39, 61	1.06	0.20	Yes	−0.09	−0.22	Yes
MYL6	Exon 6	45	0.73	−0.07	Yes	−0.42	0.00	Yes
SCML1	Exons 3, 4	149, 84	−0.74	0.10	Yes	−0.18	0.18	Yes
MAP4K4	Exon 17	231	−1.15	−0.49	Yes	−0.07	0.25	Yes
BCL2L1	Exon 2′	189	−0.51	−1.22	No	−0.42	−0.81	No
MYLK	Exon 10	204	−0.17	−0.69	No	0.20	−1.09	No
STK6	Exon 2	98	−1.25	−0.20	N/A ‡	0.08	−0.04	N/A ‡
VDU1	Exon 2	137	−1.32	−0.09	N/A §	0.00	0.21	N/A §
TP73	Exon 13	94	0.30	0.60	ND	0.04	0.25	ND

*Oligo probe e5-v8 (see Fig. 5).
†Oligo probe e5-e15 (see Fig. 5).
‡Alu repeat sequences.
§L1 repeated sequences.

Direct microarray comparison of MDA-MB-231 with MCF7 indicates that the decrease of inclusion (a negative inclusion index) is accompanied by an increase of exclusion (a positive skipping index; Table 3). To further investigate the splicing of APLP2 in these cell lines, the RNA samples were analyzed by RT-PCR using primers flanking the alternatively spliced exon 7 (Fig. 3). Products from the RT-PCR reaction were quantitated and the binary logarithm of the ratio of the inclusion form (*top*) and of the skipping form (*bottom*) was calculated (Fig. 3*C, solid columns*). By comparing with the inclusion and exclusion indexes from the microarray data (*hatched columns*), the two assays were found to be in good agreement. In six cases where the microarray indexes were above the threshold (>0.58 or less than −0.58), RT-PCR results showed the same changes with a greater number. In two cases where the microarray indexes were below the threshold (Fig. 3*C*, inclusion index of −0.06, MCF7/HMEC, two-dimensional; exclusion index of 0.32, MDA-MB-231/HMEC, two-dimensional), RT-PCR results showed either a small change (0.42) or a significant change in the same direction (0.88). It seems that a threshold of 0.58 (1.5-fold) for microarray assay is very reliable and may be a bit conservative. It also suggests that RT-PCR is a more sensitive assay. The RT-PCR assay also revealed in both cancer cell lines that a change of the inclusion form was actually accompanied by a change of the exclusion form in the opposite direction (Fig. 3*B* and *C*). Thus, both assays revealed a switch between two mutually exclusive alternative splicing events in APLP2.

HRMT1L1 encodes an hnRNP methyltransferase-like protein and is a human homologue of rat PRMT2 (protein arginine methyltransferase 2), which regulates RNA processing and maturation by modulating the activity of RNA-binding proteins (32). This gene has been recently identified as ERα coactivator (33). HRMT1L1 has a 109-nucleotide alternative exon 2 that is located before the translation start codon. When comparing with HMEC, the array data indicated an increase in exon 2 inclusion in MDA-MB-231 cells (Table 2) but no significance change in MCF7 (Table 1). Direct microarray comparison between the two cancer cell lines indicated a preference of exon 2 inclusion in MDA-MB-231 in both two-dimensional and three-dimensional conditions (Table 3). Consistent with this, RT-PCR showed the inclusion form is more prevalent in MDA-MB-231 cells than in HMEC or MCF7 cells (Fig. 4). The splicing indexes from the microarray results were compared with the values from the RT-PCR results (Fig. 4*C*). In three cases where the microarray indexes were above threshold (0.58), the RT-PCR showed the same changes with a greater number. Again, a threshold of 0.58 for microarray is completely reliable. In the other five cases where the microarray indexes were below the threshold, RT-PCR detected little changes in two cases but significant changes in three cases (Fig. 4*C*). Interestingly, the three cases that the microarray missed were all in the detection of the exclusion form (Fig. 3*C, bottom*). It seems that junction oligo e1-e3 was less effective in measuring the exclusion form. The reason for this was not yet clear, but it pointed out the importance of probing both forms concurrently on the same microarray when analyzing a single alternative exon.

An extremely complex example of multiple alternative splicing is the human *CD44* gene (Fig. 5*A*). *CD44*, encoding a cell surface adhesion molecule, has five constitutive exons (e1-e5) at the 5′ end and five constitutive exons (e15-e19) at the 3′ end. Between these two sets of exons are nine variable exons (v2-v10) that can be included or excluded in various combinations. When comparing to HMEC using microarray, both MCF7 and MDA-MB-231 showed increase of CD44v10 (oligo probe e5-v10) and CD44s (oligo probe e5-e15; Tables 1 and 2). The same comparison showed an increase of v8 inclusion (oligo probe e5-v8) in MCF7 (Table 1) and a decrease of v8 inclusion in MDA-MB-231 (Table 2). On the other hand, direct microarray comparison between the two cancer cell lines indicated

less v8-containing splice variants in MDA-MB-231 (Table 3). We carried out RT-PCR using a pair of primers, one hybridized to exon 5 and one to exon 15, to analyze the alternative splicing pattern of CD44 in HMEC, MCF7, and MDA-MB-231 cells (Fig. 5). Three major PCR products were sequenced, which corresponded to CD44v8-9-10, CD44v10, and CD44s splice variants (Fig. 5*B*). The major splice variants in HMEC are CD44v8-9-10 and CD44s; in MCF7 are CD44v8-9-10 and CD44s; and in MDA-MB-231 are CD44v10 and CD44s. The microarray data were compared with the

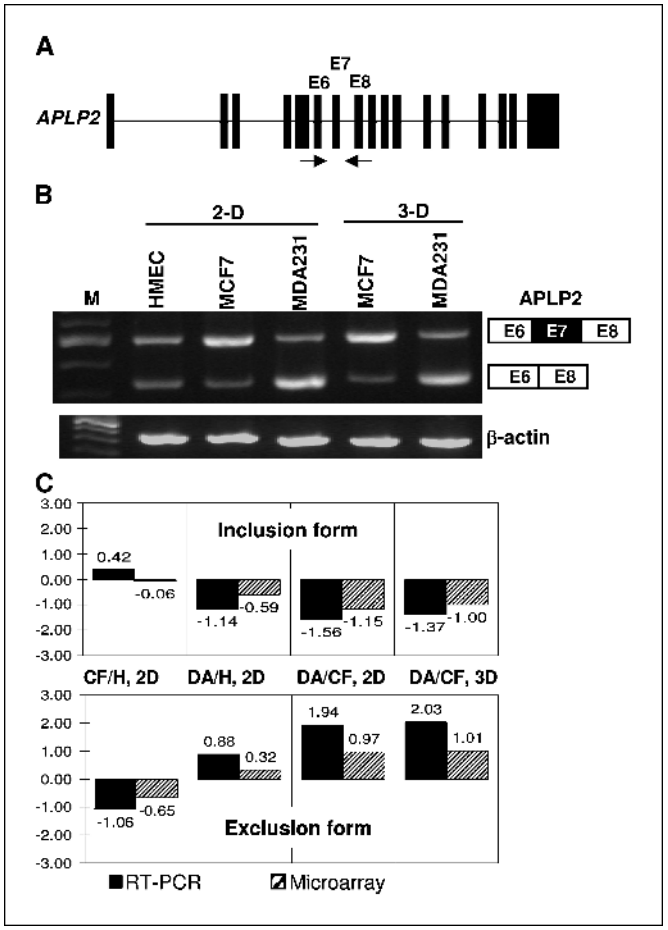

Figure 3. Alternative splicing of mRNA from the *APLP2* gene in MCF7, MDA-MB-231, and HMEC cells. *A,* exon-intron arrangement of the *APLP2* gene. *Solid bars,* exons. *Lines between exons,* introns. There are 17 exons in *APLP2* gene. The constitutive exons e6 and e8 and the alternative exon e7 are indicated. Microarray probes are situated as shown in Fig. 1*A*. *Arrows,* the primer pair used in the PCR experiment. *B,* RT-PCR assays of alternative splicing of APLP2 mRNA. Total RNA was isolated from cells grown in two-dimensional or in three-dimensional culture as indicated and reverse transcribed to cDNA using oligo(dT) and random sequence oligos. cDNA was then amplified by PCR using e6 and e8 primers, and the products were resolved in 2% agarose gels. *Top band,* exon-inclusion form; *bottom band,* exon-skipping form, as indicated on the right. cDNA was also amplified using β-actin-specific primers for comparison. *M,* DNA size marker. *C,* comparison of inclusion or exclusion indexes from the RT-PCR results (*solid columns*) and from the microarray analysis (*hatched columns*). *Top,* the inclusion index from RT-PCR experiments was calculated as $\log_2$ of the ratio between the intensity (as percentage of the total) of the inclusion form of one sample and the intensity (as percentage of the total) of the inclusion form of another sample; the inclusion index for microarray experiments was calculated by taking $\log_2$ of the ratio between exon-inclusion junctions and constitutive exons. *Bottom,* the exclusion indexes were analyzed in a similar fashion except that the exclusion forms were analyzed. *CF/H, 2D,* MCF7 two-dimensional versus HMEC two-dimensional; *DA/H, 2D,* MDA-MB-231 two-dimensional versus HMEC two-dimensional; *DA/CF, 2D,* MDA-MB-231 two-dimensional versus MCF7 two-dimensional; *DA/CF, 3D,* MDA-MB-231 three-dimensional versus MCF7 three-dimensional.

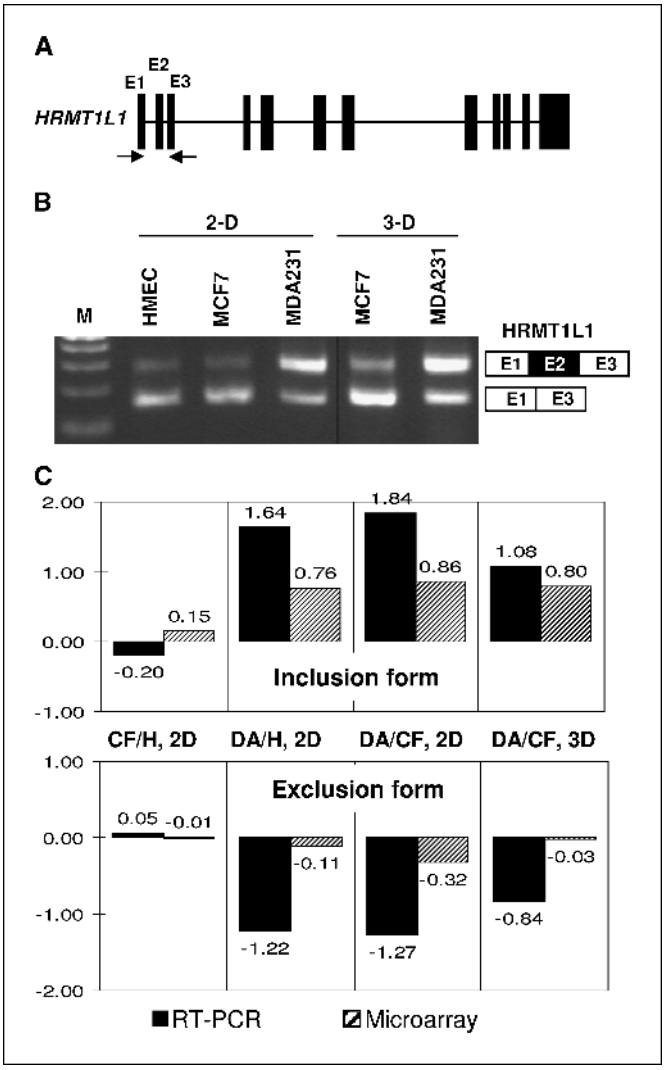

Figure 4. Alternative splicing of mRNA from the *HRMT1L1* gene in MCF7, MDB-MB-231, and HMEC cells. *A,* exon-intron arrangement of the *HRMT1L1* gene. There are 12 exons in the *HRMT1L1* gene. *B,* RT-PCR assays of alternative splicing of HRMT1L1 mRNA. *C,* comparison of inclusion or exclusion indexes from the RT-PCR results (*solid columns*) and from the microarray analysis (*hatched columns*). Samples were prepared and analyzed as described in Fig. 3.

RT-PCR results in these three major forms (Fig. 5*C*, using microarray oligo e5-e15 for the v8-9-10 form). In nine cases where the microarray indexes were above the threshold of 0.58 (an index of 0.55 in CD44v10 was included in this analysis), RT-PCR results showed the same changes with a greater number. Again, a threshold of 0.58 for microarray is completely reliable. In the other three cases where the microarray indexes were below the threshold, RT-PCR showed significant changes with two (CD44s, MDA-MB-231/MCF7, two-dimensional and three-dimensional) in the same direction and one (CD44v10, MDA-MB-231/MCF7, two-dimensional) in the opposite direction (Fig. 5*C*). Thus, even in a situation where many splice variants were produced from one gene, our oligonucleotide microarray was able to detect most of the time differences in alternative splicing.

Splicing patterns in MCF7 cell-derived tumors in nude mice. To determine whether the splicing patterns we observed in cultured cells were reflected *in vivo*, we established and analyzed

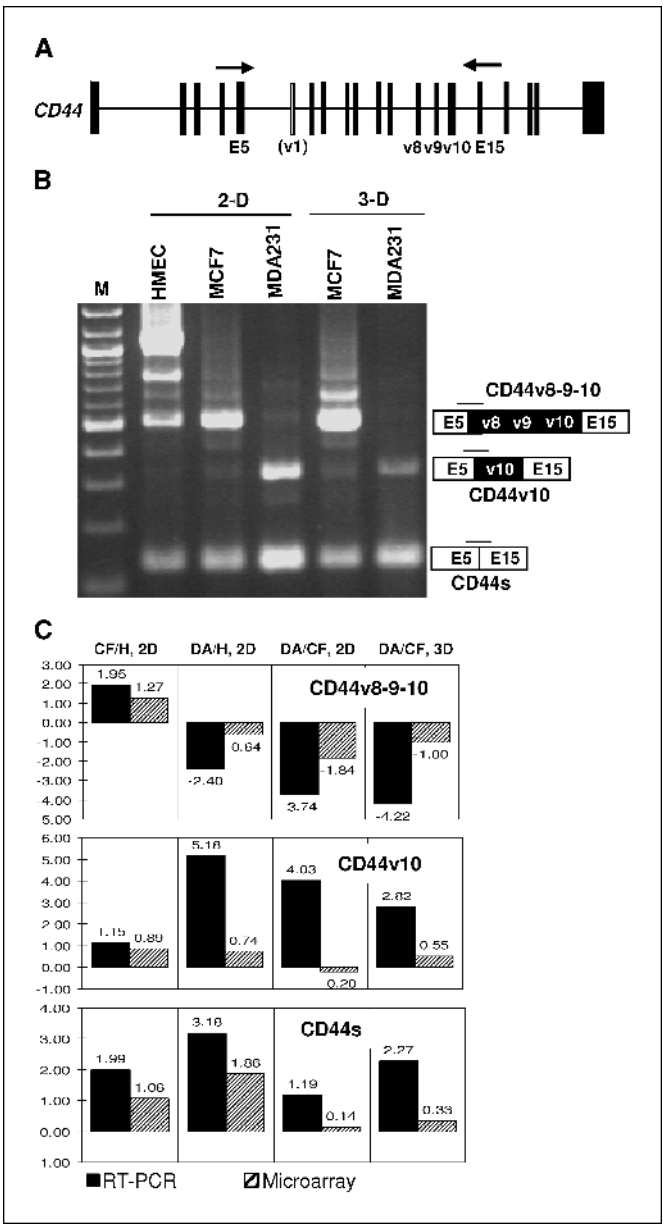

Figure 5. Alternative splicing of mRNA from the *CD44* gene in MCF7, MDA-MB-231, and HMEC cells. *A,* exon-intron arrangement of the *CD44* gene. Human *CD44* has five constitutive exons at the 5′ region (e1-e5), nine variable exons in the middle (v2-v10), and five constitutive exons at the 3′ region (e15-e19). Variable exon 1 (v1, *open box*) exists in mouse but not in human. *Arrows,* primer pair used in the RT-PCR experiments. *B,* RT-PCR assays of alternative splicing of CD44 mRNA. Samples were prepared and assayed as described in Fig. 3 except that primers specific to e5 and e15 were used in PCR. Three splice variants are depicted: CD44v8-9-10 contains v8, v9, and v10; CD44v10 contains only one variable exon, v10; CD44s does not include any variable exon. The microarray junction probe referring to CD44v8-9-10, CD44v10, or CD44s is indicated on top of the variant. *C,* comparison of inclusion or exclusion indexes of the variable exons from the RT-PCR results (*solid columns*) and from the microarray analysis (*hatched columns*). Analysis was done as described in Fig. 3 except that CD44v8-9-10 splice (*top*), CD44v10 (*middle*), and CD44s (*bottom*) were compared.

tumors derived from MCF7 cells in nude mice. MCF7 cells (2.7×10^6) were injected s.c. into nude mice. Two weeks later, the mice were sacrificed and total RNA was extracted from the excised xenograft tumor. We analyzed by RT-PCR the inclusion or exclusion of alternative exons in several genes, including *APLP2, HRMT1L1, MYL6, hnRNPA/B, ZNF207, MAP4K4*, and *SCML1*, where alternative splicing were evident in various samples. In this analysis, the ratio between the inclusion form and the exclusion/skipping form (I/S) from each gene was calculated based on the intensity of the PCR products (Fig. 6). The RT-PCR analysis showed resemblance of I/S ratio in MYL6 (inclusion of exon 6), ZNF207 (inclusion of exon 9), and hnRNPA/B (inclusion of exon 7) between the xenograft and three-dimensional samples (Fig. 6). The I/S ratios of the xenograft and of the two-dimensional samples were more divergent (Fig. 6). There were no significant splicing differences among the two-dimensional, three-dimensional, and the xenograft samples in APLP2, HRMT1L1, MAP4K4, and SCML1 (data not shown). The results indicated that alternative splicing in tumor was very similar in all examined cases to the alternative splicing in Matrigel three-dimensional culture. However, in three cases analyzed, splicing in tumor was noticeably different than splicing in flat-dish two-dimensional culture. Thus, Matrigel culture seems to be superior as an experimental model for studying *in vivo* alternative splicing, and the splicing pattern detected by microarray of the three-dimensional culture could be indicative of what occurs *in vivo*.

Discussion

In this study, we compared alternative splicing of mRNAs from 64 genes among human breast cancer cell lines and normal mammary epithelial cells using oligonucleotide microarrays and RT-PCR. The cells were cultured in flat dishes or in Matrigel where cells could grow in three dimensions. One cell line was also allowed to develop into tumor as xenografts in nude mice. The comparisons revealed splicing differences in specific genes between the cancer cells and the normal epithelial cells, between two different cancer cells, and between cells of the same type that grew in different environments. Thus, the combination of splicing-sensitive microarray and RT-PCR allowed us to identify alternative splicing events that were unique to cancer cells or regulated by the growing conditions.

DNA microarrays have been widely used to measure RNA levels as indicators for gene expression and only recently oligonucleotide

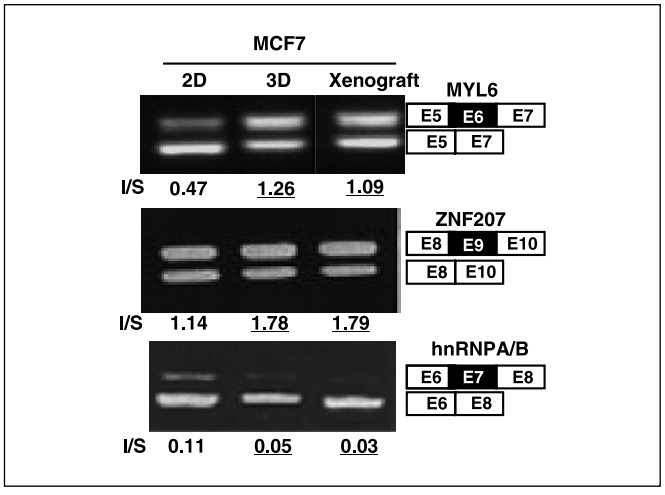

Figure 6. Alternative splicing of mRNA from three genes (*MYL6, ZNF207*, and *hnRNPA/B*) in MCF7 cells grown in two-dimensional or three-dimensional culture or as a xenograft in nude mouse. Total RNA was isolated from cells and subjected to RT-PCR assays as described in Fig. 3. PCR primers were specific to the flanking exons (*open boxes*) for each gene. *Filled box,* alternative exon: exon 6 in MYL6, exon 9 in ZNF207, and exon 7 in hnRNPA/B. The I/S ratio (*numbers below the lane*) is the ratio between the intensity of inclusion form (*top band*) and the intensity of the skipping form (*bottom band*) in each sample.

microarrays were developed to distinguish different RNA species, particularly splice variants, that were encoded by the same gene. Splicing-sensitive microarrays are used to study splicing deficiency or splicing alteration in yeast (9, 14), fly (15), mouse (16), and human (10, 11, 13, 17). This is the first time that a splicing-sensitive microarray was used to identify splicing variants that were uniquely or predominantly expressed in breast cancer cells grown under conditions that mimic the *in vivo* situation.

When analyzing the microarray data, we calculated the inclusion index and exclusion index for each alternatively spliced exon. With 1.5-fold changes (indexes >0.58 or less than −0.58 in binary logarithm) as arbitrary cutoff, ~75% of the splicing changes were confirmed by RT-PCR assays of the same RNA samples. It is worthwhile to note that in the three genes studied in detail, all 18 cases where a microarray index was above the threshold (including an index of 0.55) were in agreement with RT-PCR results (Figs. 3-5). Thus, a 50% difference as measured by microarray seemed to be a very reliable indication of a splicing change. The cutoff probably could be lowered to 25% because significant splicing changes were detected by RT-PCR in all three cases where the microarray index was 0.33 or 0.32 (Fig. 3*C*, exclusion, MDA-MB-231/HMEC, two-dimensional; Fig. 4*C*, exclusion, MDA-MB-231/MCF7, two-dimensional; Fig. 5*C*, CD44s, MDA-MB-231/MCF7, three-dimensional). Detection efficiency using our microarray is quite comparable with other studies; for example, validation rates of 70% to 85% have been reported when studying human tissue samples (13). One factor that could dampen the accuracy of the microarrays was that many alternatively spliced exons have homology to repetitive sequences like the Alu element (34). For example, we have found one Alu sequence in the alternative exon of STK6 and one L1 sequence in VDU1, suggesting that cross-hybridization of these probes occurred in the microarray. Indeed, splicing changes that were found in STK6 and VDU1 by microarray could not be verified by RT-PCR. Thus, eliminating these shortcomings would improve the accuracy in our microarray analysis.

Clearly, this work is just a beginning in the investigation of genome-wide alternative splicing changes that occur in breast cancer. The 64 genes that were assayed only represent ~0.2% of all alternatively spliced genes in human; in addition, the number of genes analyzed were too few to provide a systematic view of pathway linkages. Nevertheless, we provided summary tables in the Supplementary Data listing genes analyzed in this study whose mRNAs were spliced differentially. Supplementary Table S3 lists genes whose mRNAs were spliced differentially in both cancer cell lines versus normal HMECs, Supplementary Table S4 lists genes whose mRNAs were spliced differentially in one cancer cell line but the differential splicing was not seen in the other cancer cell line or the differential splicing was in a different type, and Supplementary Table S5 lists genes whose mRNAs were spliced differently between MDA-MB-231 and MCF7 in two-dimensional and/or in three-dimensional culture.

We detected a few splicing preferences that were associated with MCF7 and MDA-MB-231 breast cancer cell lines but not with HMEC: the inclusion of exon 7 in hnRNPA/B, the inclusion of exon 9 of RMB9, the skipping of exons 3 and 4 in FAS, and the skipping of exon 6 in MYL6 (Tables 1 and 2; Supplementary Table S3). The physiologic function of the splice variants was not investigated here; however, some of these splice variants could be interesting. For example, RBM9 (human RTA or mouse Fxh) is a Fox-1-related RNA-binding protein; it is a potent repressor of tamoxifen-mediated ER transcription (35) and capable of binding to UGCAUG sequence and regulating alternative splicing (36). RBM9 was thought to interact with ERα and to recruit corepressor complex to the receptor. The breast cancer cell lines have less exon 9–skipped form than HMEC has; exclusion of exon 9 results in a frameshift and eliminates a conserved RGG domain, which is often involved in RNA binding. The ratio between the inclusion and exclusion forms could affect the RNA binding or ER interaction by RMB9 and it would be interesting to investigate whether the change of this ratio contributes to alternative splicing and breast cancer. The splicing preference in FAS is of particular interest for cancer. FAS is a tumor necrosis factor (TNF) receptor superfamily protein that plays an important role in apoptosis. The exon-skipped form that was prevalent in MCF7 and MDA-MB-231 encodes soluble FAS that could neutralize cytotoxic factors such as TNF-α (37–39) and prevent apoptosis in breast cancer cells.

Our analysis also revealed a number of splicing differences between the two cancer cell lines of distinct tumorigenicity (HRMT1L1, APLP2, CD44, VEGF, ESR1, and EEF1D; Table 3). Although the significance of these splicing differences is not clear, one gene is worthy of comments. CD44 is a cell adhesion molecule and its splice variants are closely associated with breast and other types of cancer (21). MDA-MB-231 cells are more metastatic and invasive, suggesting that CD44s or CD44v10 plays a role in the progression and metastasis of human breast cancer. Coexpression of both CD44v10 and CD44s in HBL100 cells reduces the hemagglutinin-mediated cell adhesion and increases the migration capability in collagen-matrix gel (40). These cells also constitutively produce certain angiogenic factors and effectively promote tumorigenesis in athymic nude mice (40). Therefore, coexpression of CD44v10 and CD44s could trigger the onset of cell transformation required for breast cancer development. Knowing which splice variants of CD44 are expressed is of value to diagnose stages of breast cancer.

We also noted that the splicing pattern in tumor (as MCF7-derived xenograft in nude mice) was more comparable with the pattern seen in Matrigel-cultured cells than in flat dish–cultured cells. This indicates that Matrigel-cultured cells would be more useful for alternative splicing studies because the results are likely more relevant to what occurs *in vivo*. Cells cultured in flat dish, on the other hand, had a number of alternative splicing forms different from what were seen *in vivo*. For example, alternative splicing in MYL6, ZNF207, and hnRNPA/B in the two-dimensional culture were different than that in the three-dimensional culture or the xenografts (Fig. 6). These differences could be attributed to the involvement of extracellular matrix because extracellular matrix has been shown to regulate alternative splicing of fibronectin (41), cyclin L (42), and CD45 (43). *MYL6* encodes two alkali light chain isoforms in myosins; one includes exon 6 and is found in smooth muscle cells; the other excludes exon 6 and is found in nonmuscle cells (44). The smooth muscle myosin light chain is found up-regulated upon ethanol treatment in breast cancer T47D cells (45). Switching from the smooth muscle type to the nonmuscle type of myosin perhaps has an effect on the migration of breast cancer cells.

Documenting the splicing changes between breast cancer cells and normal cells could reveal potential roles of specific splicing variants in cancer development, progression, or metastasis. In addition, these splicing variations can also be used as tumor markers for diagnostic or prognostic evaluations in breast cancer. Thus, this study illustrates the potential of using splicing-sensitive microarray and Matrigel-cultured cells in understanding gene expression with resolution of alternative splicing in breast cancer progression.

Acknowledgments

Received 7/25/2005; revised 11/17/2005; accepted 12/12/2005.

Grant support: NIH grant GM40639 (R-J. Lin) and the City of Hope Breast Cancer Training Program (C. Li and M. Kato). Work in the Ares lab was supported by a grant from the UC Cancer Research Coordinating Committee.

The costs of publication of this article were defrayed in part by the payment of page charges. This article must therefore be hereby marked *advertisement* in accordance with 18 U.S.C. Section 1734 solely to indicate this fact.

We thank Valerie Welch (University of California Santa Cruz) for showing C. Li and M. Kato how to run microarray assays; City of Hope Functional Genomics Core Facility for providing reagents and training for some initial microarray assays; City of Hope Bioinformatics for training in GeneSpring Software; David Smith and Sean Upchurch for help with microarray data analysis; Desiree Crow for preparing MCF7 xenograft; the Lin lab members for comments and suggestions; Kristine Justus for reviewing the manuscript; and X.D. Fu (University of California San Diego) for insightful comments on the manuscript.

References

1. Venables JP. Aberrant and alternative splicing in cancer. Cancer Res 2004;64:7647–54.
2. Miki Y, Swensen J, Shattuck-Eidens D, et al. A strong candidate for the breast and ovarian cancer susceptibility gene BRCA1. Science 1994;266:66–71.
3. Orban TI, Olah E. Emerging roles of BRCA1 alternative splicing. Mol Pathol 2003;56:191–7.
4. Mazoyer S, Puget N, Perrin-Vidoz L, et al. A BRCA1 nonsense mutation causes exon skipping. Am J Hum Genet 1998;62:713–5.
5. Liu HX, Cartegni L, Zhang MQ, Krainer AR. A mechanism for exon skipping caused by nonsense or missense mutations in BRCA1 and other genes. Nat Genet 2001;27:55–8.
6. Manley JL, Tacke R. SR proteins and splicing control. Genes Dev 1996;10:1569–79.
7. Hastings ML, Krainer AR. Pre-mRNA splicing in the new millennium. Curr Opin Cell Biol 2001;13:302–9.
8. Stickeler E, Kittrell F, Medina D, Berget SM. Stage-specific changes in SR splicing factors and alternative splicing in mammary tumorigenesis. Oncogene 1999;18:3574–82.
9. Clark TA, Sugnet CW, Ares M, Jr. Genomewide analysis of mRNA processing in yeast using splicing-specific microarrays. Science 2002;296:907–10.
10. Yeakley JM, Fan JB, Doucet D, et al. Profiling alternative splicing on fiber-optic arrays. Nat Biotechnol 2002;20:353–8.
11. Johnson JM, Castle J, Garrett-Engele P, et al. Genome-wide survey of human alternative pre-mRNA splicing with exon junction microarrays. Science 2003;302:2141–4.
12. Wang H, Hubbell E, Hu JS, et al. Gene structure-based splice variant deconvolution using a microarray platform. Bioinformatics 2003;19 Suppl 1:i315–22.
13. Le K, Mitsouras K, Roy M, et al. Detecting tissue-specific regulation of alternative splicing as a qualitative change in microarray data. Nucleic Acids Res 2004;32:e180.
14. Burckin T, Nagel R, Mandel-Gutfreund Y, et al. Exploring functional relationships between components of the gene expression machinery. Nat Struct Mol Biol 2005;12:175–82.
15. Blanchette M, Green RE, Brenner SE, Rio DC. Global analysis of positive and negative pre-mRNA splicing regulators in Drosophila. Genes Dev 2005;19:1306–14.
16. Pan Q, Shai O, Misquitta C, et al. Revealing global regulatory features of mammalian alternative splicing using a quantitative microarray platform. Mol Cell 2004;16:929–41.
17. Relogio A, Ben-Dov C, Baum M, et al. Alternative splicing microarrays reveal functional expression of neuron-specific regulators in Hodgkin lymphoma cells. J Biol Chem 2005;280:4779–84.
18. Mukhopadhyay R, Theriault RL, Price JE. Increased levels of α6 integrins are associated with the metastatic phenotype of human breast cancer cells. Clin Exp Metastasis 1999;17:325–32.
19. Shafie SM, Liotta LA. Formation of metastasis by human breast carcinoma cells (MCF-7) in nude mice. Cancer Lett 1980;11:81–7.
20. Srinivasan K, Shiue L, Hayes JD, et al. Detection and measurement of alternative splicing using splicing-sensitive microarrays. Methods 2005;37:345–59.
21. Naot D, Sionov RV, Ish-Shalom D. CD44: structure, function, and association with the malignant process. Adv Cancer Res 1997;71:241–319.
22. Boutros R, Bailey AM, Wilson SH, Byrne JA. Alternative splicing as a mechanism for regulating 14–3-3 binding: interactions between hD53 (TPD52L1) and 14–3-3 proteins. J Mol Biol 2003;332:675–87.
23. Kleinman HK, McGarvey ML, Liotta LA, et al. Isolation and characterization of type IV procollagen, laminin, and heparan sulfate proteoglycan from the EHS sarcoma. Biochemistry 1982;21:6188–93.
24. Wolf K, Mazo I, Leung H, et al. Compensation mechanism in tumor cell migration: mesenchymal-amoeboid transition after blocking of pericellular proteolysis. J Cell Biol 2003;160:267–77.
25. Sahai E, Marshall CJ. Differing modes of tumour cell invasion have distinct requirements for Rho/ROCK signalling and extracellular proteolysis. Nat Cell Biol 2003;5:711–9.
26. Cukierman E, Pankov R, Stevens DR, Yamada KM. Taking cell-matrix adhesions to the third dimension. Science 2001;294:1708–12.
27. Glondu M, Liaudet-Coopman E, Derocq D, et al. Down-regulation of cathepsin-D expression by antisense gene transfer inhibits tumor growth and experimental lung metastasis of human breast cancer cells. Oncogene 2002;21:5127–34.
28. Kirshner J, Chen CJ, Liu P, Huang J, Shively JE. CEACAM1–4S, a cell-cell adhesion molecule, mediates apoptosis and reverts mammary carcinoma cells to a normal morphogenic phenotype in a 3D culture. Proc Natl Acad Sci U S A 2003;100:521–6.
29. Suzuki T, Ando K, Isohara T, et al. Phosphorylation of Alzheimer β-amyloid precursor-like proteins. Biochemistry 1997;36:4643–9.
30. Adlerz L, Beckman M, Holback S, et al. Accumulation of the amyloid precursor-like protein APLP2 and reduction of APLP1 in retinoic acid-differentiated human neuroblastoma cells upon curcumin-induced neurite retraction. Brain Res Mol Brain Res 2003;119:62–72.
31. Sandbrink R, Masters CL, Beyreuther K. Similar alternative splicing of a non-homologous domain in β A4-amyloid protein precursor-like proteins. J Biol Chem 1994;269:14227–34.
32. Scott HS, Antonarakis SE, Lalioti MD, et al. Identification and characterization of two putative human arginine methyltransferases (HRMT1L1 and HRMT1L2). Genomics 1998;48:330–40.
33. Qi C, Chang J, Zhu Y, et al. Identification of protein arginine methyltransferase 2 as a coactivator for estrogen receptor α. J Biol Chem 2002;277:28624–30.
34. Lev-Maor G, Sorek R, Shomron N, Ast G. The birth of an alternatively spliced exon: 3′ splice-site selection in Alu exons. Science 2003;300:1288–91.
35. Norris JD, Fan D, Sherk A, McDonnell DP. A negative coregulator for the human ER. Mol Endocrinol 2002;16:459–68.
36. Nakahata S, Kawamoto S. Tissue-dependent isoforms of mammalian Fox-1 homologs are associated with tissue-specific splicing activities. Nucleic Acids Res 2005;33:2078–89.
37. Screaton GR, Xu XN, Olsen AL, et al. LARD: a new lymphoid-specific death domain containing receptor regulated by alternative pre-mRNA splicing. Proc Natl Acad Sci U S A 1997;94:4615–9.
38. Grenet J, Valentine V, Kitson J, et al. Duplication of the DR3 gene on human chromosome 1p36 and its deletion in human neuroblastoma. Genomics 1998;49:385–93.
39. Ruberti G, Cascino I, Papoff G, Eramo A. Fas splicing variants and their effect on apoptosis. Adv Exp Med Biol 1996;406:125–34.
40. Iida N, Bourguignon LY. Coexpression of CD44 variant (v10/ex14) and CD44S in human mammary epithelial cells promotes tumorigenesis. J Cell Physiol 1997;171:152–60.
41. Blaustein M, Pelisch F, Coso OA, et al. Mammary epithelial-mesenchymal interaction regulates fibronectin alternative splicing via phosphatidylinositol 3-kinase. J Biol Chem 2004;279:21029–37.
42. Sgambato V, Minassian R, Nairn AC, Hyman SE. Regulation of ania-6 splice variants by distinct signaling pathways in striatal neurons. J Neurochem 2003;86:153–64.
43. Tchilian EZ, Beverley PC. CD45 in memory and disease. Arch Immunol Ther Exp (Warsz) 2002;50:85–93.
44. Lenz S, Lohse P, Seidel U, Arnold HH. The alkali light chains of human smooth and nonmuscle myosins are encoded by a single gene. Tissue-specific expression by alternative splicing pathways. J Biol Chem 1989;264:9009–15.
45. Zhu Y, Lin H, Wang M, et al. Up-regulation of transcription of smooth muscle myosin alkali light chain by ethanol in human breast cancer cells. Int J Oncol 2001;18:1299–305.